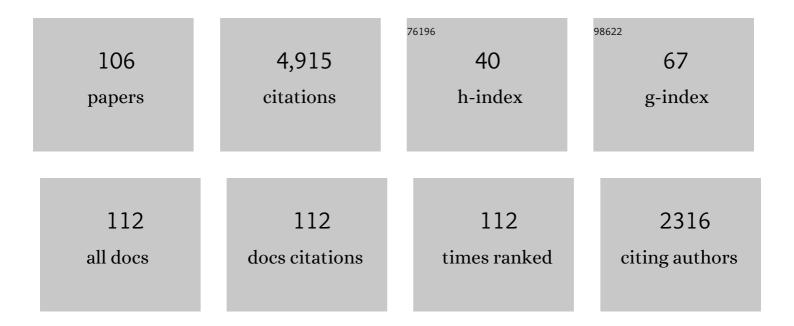
List of Publications by Year in descending order

Source: https://exaly.com/author-pdf/2659363/publications.pdf

Version: 2024-02-01



#	Article	IF	CITATIONS
1	Late Paleoproterozoic to early Mesoproterozoic Dongchuan Group in Yunnan, SW China: Implications for tectonic evolution of the Yangtze Block. Precambrian Research, 2010, 182, 57-69.	1.2	325
2	Detrital zircon U–Pb geochronological and Lu–Hf isotopic constraints on the Precambrian magmatic and crustal evolution of the western Yangtze Block, SW China. Precambrian Research, 2009, 172, 99-126.	1.2	309
3	OIB-like, heterogeneous mantle sources of Permian basaltic magmatism in the western Tarim Basin, NW China: Implications for a possible Permian large igneous province. Lithos, 2009, 113, 583-594.	0.6	249
4	Compositions of chromite, associated minerals, and parental magmas of podiform chromite deposits: The role of slab contamination of asthenospheric melts in suprasubduction zone environments. Gondwana Research, 2014, 26, 262-283.	3.0	228
5	Geochemistry of the Meso- to Neoproterozoic basic–acid rocks from Hunan Province, South China: implications for the evolution of the western Jiangnan orogen. Precambrian Research, 2004, 135, 79-103.	1.2	191
6	Genetic types, mineralization styles, and geodynamic settings of Mesozoic tungsten deposits in South China. Journal of Asian Earth Sciences, 2017, 137, 109-140.	1.0	146
7	Geochemistry of Meso- and Neoproterozoic mafic-ultramafic rocks from northern Guangxi, China: Arc or plume magmatism?. Geochemical Journal, 2004, 38, 139-152.	0.5	140
8	Constraints of in situ zircon and cassiterite U–Pb, molybdenite Re–Os and muscovite 40Ar–39Ar ages on multiple generations of granitic magmatism and related W–Sn mineralization in the Wangxianling area, Nanling Range, South China. Ore Geology Reviews, 2015, 65, 1021-1042.	1.1	132
9	Sulfide Saturation and Magma Emplacement in the Formation of the Permian Huangshandong Ni-Cu Sulfide Deposit, Xinjiang, Northwestern China. Economic Geology, 2013, 108, 1833-1848.	1.8	127
10	Permian alkaline granites in the Erenhot–Hegenshan belt, northern Inner Mongolia, China: Model of generation, time of emplacement and regional tectonic significance. Journal of Asian Earth Sciences, 2015, 97, 320-336.	1.0	116
11	In-situ LA-ICP-MS trace elemental analyses of magnetite: Fe–Ti–(V) oxide-bearing mafic–ultramafic layered intrusions of the Emeishan Large Igneous Province, SW China. Ore Geology Reviews, 2015, 65, 853-871.	1.1	90
12	An improved Carius tube technique for determination of low concentrations of Re and Os in pyrites. Journal of Analytical Atomic Spectrometry, 2010, 25, 585.	1.6	85
13	Post-accretionary permian granitoids in the Chinese Altai orogen: Geochronology, petrogenesis and tectonic implications. Numerische Mathematik, 2014, 314, 80-109.	0.7	83
14	Re–Os isotopic ages of pyrite and chemical composition of magnetite from the Cihai magmatic–hydrothermal Fe deposit, NW China. Mineralium Deposita, 2013, 48, 925-946.	1.7	74
15	First Reliable <scp>Re–Os</scp> Ages of Pyrite and Stable Isotope Compositions of <scp>F</scp> e(â€ <scp>C</scp> u) Deposits in the <scp>H</scp> ami Region, <scp>E</scp> astern <scp>T</scp> ianshan <scp>O</scp> rogenic <scp>B</scp> elt, <scp>NW C</scp> hina. Resource Geology, 2013. 63. 166-187.	0.3	74
16	Origin of PGE-Poor and Cu-Rich Magmatic Sulfides from the Kalatongke Deposit, Xinjiang, Northwest China. Economic Geology, 2012, 107, 481-506.	1.8	72
17	In-situ LA-ICP-MS trace elemental analyses of magnetite: Cu-(Au, Fe) deposits in the Khetri copper belt in Rajasthan Province, NW India. Ore Geology Reviews, 2015, 65, 929-939.	1.1	70
18	Generation and evolution of siliceous high magnesium basaltic magmas in the formation of the Permian Huangshandong intrusion (Xinjiang, NW China). Lithos, 2013, 162-163, 128-139.	0.6	69

#	Article	IF	CITATIONS
19	An improved digestion technique for determination of platinum group elements in geological samples. Journal of Analytical Atomic Spectrometry, 2011, 26, 1900.	1.6	66
20	Petrogenesis of the Archean tonalite–trondhjemite–granodiorite (TTG) and granites in the Lushan area, southern margin of the North China Craton: Implications for crustal accretion and transformation. Precambrian Research, 2014, 255, 514-537.	1.2	66
21	In-situ LA–ICP-MS trace elemental analyses of magnetite: The late Palaeoproterozoic Sokoman Iron Formation in the Labrador Trough, Canada. Ore Geology Reviews, 2015, 65, 917-928.	1.1	66
22	Constraints of detrital zircon U–Pb ages and Hf isotopes on the provenance of the Triassic Yidun Group and tectonic evolution of the Yidun Terrane, Eastern Tibet. Sedimentary Geology, 2013, 289, 74-98.	1.0	64
23	Age and composition of granulite and pyroxenite xenoliths in Hannuoba basalts reflect Paleogene underplating beneath the North China Craton. Chemical Geology, 2009, 264, 266-280.	1.4	63
24	In-situ LA-ICP-MS trace elemental analyses of magnetite and Re–Os dating of pyrite: The Tianhu hydrothermally remobilized sedimentary Fe deposit, NW China. Ore Geology Reviews, 2015, 65, 900-916.	1.1	63
25	Petrogenesis and tectonic implications of the Triassic volcanic rocks in the northern Yidun Terrane, Eastern Tibet. Lithos, 2013, 175-176, 285-301.	0.6	62
26	In-situ elemental and isotopic compositions of apatite and zircon from the Shuikoushan and Xihuashan granitic plutons: Implication for Jurassic granitoid-related Cu-Pb-Zn and W mineralization in the Nanling Range, South China. Ore Geology Reviews, 2018, 93, 382-403.	1.1	60
27	In-situ LA-ICP-MS trace element analyses of scheelite and wolframite: Constraints on the genesis of veinlet-disseminated and vein-type tungsten deposits, South China. Ore Geology Reviews, 2018, 99, 166-179.	1.1	59
28	The Early Jurassic tectono-magmatic events in southern Jiangxi and northern Guangdong provinces, SE China: Constraints from the SHRIMP zircon U–Pb dating. Journal of Asian Earth Sciences, 2010, 39, 408-422.	1.0	58
29	Crustal evolution of the Eastern Block in the North China Craton: Constraints from zircon U–Pb geochronology and Lu–Hf isotopes of the Northern Liaoning Complex. Precambrian Research, 2016, 275, 35-47.	1.2	58
30	Heterogeneous mantle source and magma differentiation of quaternary arc-like volcanic rocks from Tengchong, SE margin of the Tibetan Plateau. Contributions To Mineralogy and Petrology, 2012, 163, 841-860.	1.2	56
31	Geochemistry of magnetite from Proterozoic Fe-Cu deposits in the Kangdian metallogenic province, SW China. Mineralium Deposita, 2015, 50, 795-809.	1.7	55
32	Partitioning of the Cretaceous Pan-Yangtze Basin in the central South China Block by exhumation of the Xuefeng Mountains during a transition from extensional to compressional tectonics?. Gondwana Research, 2014, 25, 1644-1659.	3.0	49
33	Mineralogical constraints on the genesis of W–Nb–Ta mineralization in the Laiziling granite (Xianghualing district, south China). Ore Geology Reviews, 2018, 95, 695-712.	1.1	48
34	Magma mixing in the genesis of the Kalatongke dioritic intrusion: Implications for the tectonic switch from subduction to post-collision, Chinese Altay, NW China. Lithos, 2013, 162-163, 236-250.	0.6	47
35	In situ Sr isotope analysis of apatite by LA-MC-ICPMS: constraints on the evolution of ore fluids of the Yinachang Fe-Cu-REE deposit, Southwest China. Mineralium Deposita, 2015, 50, 871-884.	1.7	47
36	Fractionation characteristics of rare earth elements (REEs) linked with secondary Fe, Mn, and Al minerals in soils. Acta Geochimica, 2016, 35, 329-339.	0.7	45

#	Article	IF	CITATIONS
37	Neoproterozoic chromite-bearing high-Mg diorites in the western part of the Jiangnan orogen, southern China: Geochemistry, petrogenesis and tectonic implications. Lithos, 2014, 200-201, 35-48.	0.6	44
38	Geochemistry and Si–O–Fe isotope constraints on the origin of banded iron formations of the Yuanjiacun Formation, Lvliang Group, Shanxi, China. Ore Geology Reviews, 2014, 57, 288-298.	1.1	43
39	Origin of the Muguayuan veinlet-disseminated tungsten deposit, South China: Constraints from in-situ trace element analyses of scheelite. Ore Geology Reviews, 2018, 99, 180-194.	1.1	43
40	Open magma chamber processes in the formation of the Permian Baima mafic–ultramafic layered intrusion, SW China. Lithos, 2014, 184-187, 194-208.	0.6	42
41	In-situ LA–ICP–MS trace elements analysis of magnetite: The Fenghuangshan Cu–Fe–Au deposit, Tongling, Eastern China. Ore Geology Reviews, 2016, 72, 746-759.	1.1	39
42	Zircon Alteration as a Proxy for Rare Earth Element Mineralization Processes in Carbonatite-Nordmarkite Complexes of the Mianning-Dechang Rare Earth Element Belt, China. Economic Geology, 2019, 114, 719-744.	1.8	39
43	LA-ICP-MS U Pb geochronology of wolframite by combining NIST series and common lead-bearing MTM as the primary reference material:Implications for metallogenesis of South China. Gondwana Research, 2020, 83, 217-231.	3.0	39
44	Chalcophile elemental compositions and origin of the Tuwu porphyry Cu deposit, NW China. Ore Geology Reviews, 2015, 66, 403-421.	1.1	37
45	The Pengguan tectonic dome of Longmen Mountains, Sichuan Province: Mesozoic denudation of a Neoproterozoic magmatic arc-basin system. Science in China Series D: Earth Sciences, 2008, 51, 1545-1559.	0.9	36
46	Origin of the volcanic-hosted Yamansu Fe deposit, Eastern Tianshan, NW China: constraints from pyrite Re-Os isotopes, stable isotopes, and in situ magnetite trace elements. Mineralium Deposita, 2018, 53, 1039-1060.	1.7	36
47	High water contents of magmas and extensive fluid exsolution during the formation of the Yulong porphyry Cu-Mo deposit, eastern Tibet. Journal of Asian Earth Sciences, 2019, 176, 168-183.	1.0	36
48	Platinum-group elements, zircon Hf-O isotopes, and mineralogical constraints on magmatic evolution of the Pulang porphyry Cu-Au system, SW China. Gondwana Research, 2018, 62, 163-177.	3.0	34
49	The role of hydrothermal alteration in tungsten mineralization at the Dahutang tungsten deposit, South China. Ore Geology Reviews, 2018, 95, 1008-1027.	1.1	33
50	Early Precambrian tectonothermal events of the North China Craton: Constraints from in situ detrital zircon U-Pb, Hf and O isotopic compositions in Tietonggou Formation. Science Bulletin, 2013, 58, 3760-3770.	1.7	32
51	Introduction to the special issue of Mesozoic W-Sn deposits in South China. Ore Geology Reviews, 2018, 101, 432-436.	1.1	32
52	Petrogenesis of the 2.1Ga Lushan garnet-bearing quartz monzonite on the southern margin of the North China Craton and its tectonic implications. Precambrian Research, 2015, 256, 241-255.	1.2	31
53	Magma mixing recorded by Sr isotopes of plagioclase from dacites of the Quaternary Tengchong volcanic field, SE Tibetan Plateau. Journal of Asian Earth Sciences, 2015, 98, 1-17.	1.0	31
54	The Design of Reâ€usable <scp>C</scp> arius Tubes for the Determination of Rhenium, Osmium and Platinumâ€Group Elements in Geological Samples. Geostandards and Geoanalytical Research, 2013, 37, 345-351.	1.7	29

#	Article	IF	CITATIONS
55	In situ low-U garnet U-Pb dating by LA-SF-ICP-MS and its application in constraining the origin of Anji skarn system combined with Ar-Ar dating and Pb isotopes. Ore Geology Reviews, 2021, 130, 103970.	1.1	29
56	Constraints of Sr isotopic compositions of apatite and carbonates on the origin of Fe and Cu mineralizing fluids in the Lala Fe-Cu-(Mo, LREE) deposit, SW China. Ore Geology Reviews, 2014, 61, 96-106.	1.1	28
57	Neoproterozoic granitoids from the Phan Si Pan belt, Northwest Vietnam: Implication for the tectonic linkage between Northwest Vietnam and the Yangtze Block. Precambrian Research, 2018, 309, 212-230.	1.2	27
58	Mercury isotope constraints on the source for sediment-hosted lead-zinc deposits in the Changdu area, southwestern China. Mineralium Deposita, 2018, 53, 339-352.	1.7	27
59	The origin of the carbonate-hosted Huize Zn–Pb–Ag deposit, Yunnan province, SW China: constraints from the trace element and sulfur isotopic compositions of pyrite. Mineralogy and Petrology, 2019, 113, 369-391.	0.4	25
60	Comment on "Neoproterozoic granitoids in South China: crustal melting above a mantle plume at ca. 825Ma?―by Xian-Hua Li et al. [Precambrian Res. 122 (2003) 45–83]. Precambrian Research, 2004, 132, 401-403.	1.2	24
61	Timing and genesis of Cu–(Au) mineralization in the Khetri Copper Belt, northwestern India: constraints from in situ U–Pb ages and Sm–Nd isotopes of monazite-(Ce). Mineralium Deposita, 2019, 54, 553-568.	1.7	23
62	Re-Os dating of galena and sphalerite from lead-zinc sulfide deposits in Yunnan Province, SW China. Journal of Earth Science (Wuhan, China), 2015, 26, 343-351.	1.1	22
63	Oscillatory Sr isotopic signature in plagioclase megacrysts from the Damiao anorthosite complex, North China: Implication for petrogenesis of massif-type anorthosite. Chemical Geology, 2015, 393-394, 1-15.	1.4	22
64	Disturbance of the Sm-Nd isotopic system by metasomatic alteration: A case study of fluorapatite from the Sin Quyen Cu-LREE-Au deposit, Vietnam. American Mineralogist, 2018, 103, 1487-1496.	0.9	22
65	Multistage Evolution of the Neoarchean (ca. 2.7 Ga) Igarapé Cinzento (GT-46) Iron Oxide Copper-Gold Deposit, Cinzento Shear Zone, Carajás Province, Brazil. Economic Geology, 2019, 114, 1-34.	1.8	22
66	Geochemistry, in-situ Sr-Nd-Hf-O isotopes, and mineralogical constraints on origin and magmatic-hydrothermal evolution of the Yulong porphyry Cu Mo deposit, Eastern Tibet. Gondwana Research, 2019, 76, 98-114.	3.0	19
67	Rare Earth Element and Trace Element Features of Goldâ€bearing Pyrite in the Jinshan Gold Deposit, Jiangxi Province. Acta Geologica Sinica, 2010, 84, 614-623.	0.8	18
68	Heterogeneous Os isotope compositions in the Kalatongke sulfide deposit, NW China: the role of crustal contamination. Mineralium Deposita, 2012, 47, 731-738.	1.7	18
69	Magmatic evolution and W-Sn-U-Nb-Ta mineralization of the Mesozoic Jiulongnao granitic complex, Nanling Range, South China. Ore Geology Reviews, 2018, 94, 414-434.	1.1	18
70	Hydrothermal Alteration, Fluid Evolution, and Re-Os Geochronology of the Grota Funda Iron Oxide Copper-Gold Deposit, Carajás Province (Pará State), Brazil. Economic Geology, 2018, 113, 1769-1794.	1.8	18
71	Revisiting platinum group elements of Late Permian coals from western Guizhou Province, SW China. International Journal of Coal Geology, 2008, 75, 189-193.	1.9	15
72	Sulfur and lead isotopic variations in the giant Yulong porphyry Cu (Mo Au) deposit from the eastern Tibetan Plateau: Implications for origins of S and Pb, and metal precipitation. Journal of Geochemical Exploration, 2019, 197, 70-83.	1.5	15

#	Article	IF	CITATIONS
73	Tectonic Evolution and Paleoposition of the Baoshan and Lincang Blocks of West Yunnan During the Paleozoic. Tectonics, 2020, 39, e2019TC006028.	1.3	15
74	Evidence of metasomatism in the interior of Vesta. Nature Communications, 2020, 11, 1289.	5.8	15
75	The relationship between stratabound Pb–Zn–Ag and porphyry–skarn Mo mineralization in the Laochang deposit, southwestern China: Constraints from pyrite Re-Os isotope, sulfur isotope, and trace element data. Journal of Geochemical Exploration, 2018, 194, 218-238.	1.5	14
76	Compression-extension transition of continental crust in a subduction zone: A parametric numerical modeling study with implications on Mesozoic-Cenozoic tectonic evolution of the Cathaysia Block. PLoS ONE, 2017, 12, e0171536.	1.1	13
77	Two-tiered magmatic-hydrothermal and skarn origin of magnetite from Gol-Gohar iron ore deposit of SE Iran: In-situ LA–ICP-MS analyses. Ore Geology Reviews, 2018, 102, 639-653.	1.1	13
78	Origin and evolution of ore-forming fluids in a tungsten mineralization system, Middle Jiangnan orogenic belt, South China: Constraints from in-situ LA-ICP-MS analyses of scheelite. Ore Geology Reviews, 2020, 127, 103806.	1.1	13
79	Two reliable calibration methods for accurate <i>in situ</i> U–Pb dating of scheelite. Journal of Analytical Atomic Spectrometry, 2022, 37, 358-368.	1.6	13
80	Evaluation of sample dissolution method for Sm-Nd isotopic analysis of scheelite. Journal of Analytical Atomic Spectrometry, 2012, 27, 509.	1.6	12
81	Origin and implications of troilite-orthopyroxene intergrowths in the brecciated diogenite Northwest Africa 7183. Geochimica Et Cosmochimica Acta, 2018, 220, 125-145.	1.6	12
82	Cenozoic basalts in SE China: Chalcophile element geochemistry, sulfide saturation history, and source heterogeneity. Lithos, 2017, 282-283, 215-227.	0.6	11
83	Germanium in Magnetite: A Preliminary Review. Acta Geologica Sinica, 2017, 91, 711-726.	0.8	10
84	The role of early sulfide saturation in the formation of the Yulong porphyry Cu-Mo deposit: Evidence from mineralogy of sulfide melt inclusions and platinum-group element geochemistry. Ore Geology Reviews, 2020, 124, 103644.	1.1	9
85	Trace and minor elements in sulfides from the Lengshuikeng Ag–Pb–Zn deposit, South China: A LA–ICP–MS study. Ore Geology Reviews, 2022, 141, 104663.	1.1	9
86	Platinum-group element geochemistry of intraplate basalts from the Aleppo Plateau, NW Syria. Geological Magazine, 2013, 150, 497-508.	0.9	8
87	Trace element composition of magnetite from the Xinqiao Fe–S(–Cu–Au) deposit, Tongling, Eastern China: constraints on fluid evolution and ore genesis. Acta Geochimica, 2018, 37, 639-654.	0.7	8
88	In situ Pb-Pb isotopic dating of sulfides from hydrothermal deposits: a case study of the Lala Fe-Cu deposit, SW China. Mineralium Deposita, 2019, 54, 671-682.	1.7	8
89	In situ LA-ICP-MS analyses of mica and wolframite from the Maoping tungsten deposit, southern Jiangxi, China. Acta Geochimica, 2020, 39, 811-829.	0.7	8
90	In situ LA ICP-MS analysis of trace elements in scheelite from the Xuefeng Uplift Belt, South China and its metallogenic implications. Ore Geology Reviews, 2021, 133, 104097.	1.1	8

#	Article	IF	CITATIONS
91	Episodic Archean crustal accretion in the North China Craton: Insights from integrated zircon U-Pb-Hf-O isotopes of the Southern Jilin Complex, northeast China. Precambrian Research, 2021, 358, 106150.	1.2	8
92	Re–Os isotopic and platinum group elemental constraints on the genesis of the Xiadong ophiolitic complex, Eastern Xinjiang, NW China. Gondwana Research, 2015, 27, 629-648.	3.0	6
93	Constraints of molybdenite Re–Os and scheelite Sm–Nd ages on mineralization time of the Kukaazi Pb–Zn–Cu–W deposit, Western Kunlun, NW China. Acta Geochimica, 2018, 37, 47-59.	0.7	6
94	Trace element characteristics of magnetite: Constraints on the genesis of the Lengshuikeng Ag–Pb–Zn deposit, China. Ore Geology Reviews, 2021, 129, 103943.	1.1	6
95	Magma evolution leading to veinlet-disseminated tungsten mineralization at the Muguayuan deposit: In-situ analysis of igneous minerals. Ore Geology Reviews, 2021, 138, 104406.	1.1	4
96	Re-Os isotope system of sulfide from the Fule carbonate-hosted Pb-Zn deposit, SW China: Implications for Re-Os dating of Pb-Zn mineralization. Ore Geology Reviews, 2020, 121, 103558.	1.1	3
97	Vesuvianite: A potential U-Pb geochronometer for skarn mineralizationa case study of tungsten and tin deposits in South China. Chemical Geology, 2022, 607, 121017.	1.4	3
98	Determination of rhenium and osmium by ICP-MS for galena and sphalerite. Acta Geochimica, 2016, 35, 43-49.	0.7	2
99	In Situ Trace Elemental Analyses of Scheelite from the Chuankou Deposit, South China: Implications for Ore Genesis. Minerals (Basel, Switzerland), 2020, 10, 1007.	0.8	2
100	Mantle-Derived Noble Gas Isotopes in the Ore-Forming Fluid of Xingluokeng W-Mo Deposit, Fujian Province. Minerals (Basel, Switzerland), 2022, 12, 595.	0.8	2
101	Re–Os dating of molybdenite via improved alkaline fusion. Journal of Analytical Atomic Spectrometry, 2021, 36, 64-69.	1.6	1
102	Application of low-temperature thermochronology on ore deposits preservation framework in South China: a review. Acta Geochimica, 2022, 41, 165-184.	0.7	1
103	Correlation between South China and India and development of double rift systems in the South China–India Duo during late Neoproterozoic time. Bulletin of the Geological Society of America, 2023, 135, 351-366.	1.6	1
104	U–Pb geochronology and trace-element composition of zircons from the Jinchang Au–Ni deposit, SW China, and their implications for tectonics. Geological Magazine, 2021, 158, 1269-1288.	0.9	0
105	Fluid-rock interaction of the early Cambrian black shale in the South China Block: Implications for low-temperature mineralisation. Ore Geology Reviews, 2021, 131, 104030.	1.1	0
106	Mafic-ultramafic intrusion formed by multi-stage evolution of hydrous basaltic melts. Bulletin of the Geological Society of America, 0, , .	1.6	0